ACS APPLIED MATERIALS & INTERFACES

Research Article

www.acsami.org

Membrane/Mediator-Free Rechargeable Enzymatic Biofuel Cell Utilizing Graphene/Single-Wall Carbon Nanotube Cogel Electrodes

Alan S. Campbell,[†] Yeon Joo Jeong,[‡] Steven M. Geier,[‡] Richard R. Koepsel,[§] Alan J. Russell,*[,†,§,∥,⊥] and Mohammad F. Islam*[,‡]

[†]Department of Biomedical Engineering, Carnegie Mellon University, 5000 Forbes Avenue, Pittsburgh, Pennsylvania 15213, United States

[‡]Department of Materials Science & Engineering, Carnegie Mellon University, 5000 Forbes Avenue, Pittsburgh, Pennsylvania 15213, United States

[§]The Institute for Complex Engineered Systems, Carnegie Mellon University, 5000 Forbes Avenue, Pittsburgh, Pennsylvania 15213, United States

[∥]Disruptive Health Technology Institute, Carnegie Mellon University, 5000 Forbes Avenue, Pittsburgh, Pennsylvania 15213, United States

[⊥]Department of Biological Sciences, Carnegie Mellon University, 5000 Forbes Avenue, Pittsburgh, Pennsylvania 15213, United States

Supporting Information

ABSTRACT: Enzymatic biofuel cells (EBFCs) utilize enzymes to convert chemical energy present in renewable biofuels into electrical energy and have shown much promise in the continuous powering of implantable devices. Currently, however, EBFCs are greatly limited in terms of power and operational stability with a majority of reported improvements requiring the inclusion of potentially toxic and unstable electron transfer mediators or multicompartment systems separated by a semipermeable membrane resulting in complicated setups. We report on the development of a simple, membrane/mediator-free EBFC utilizing novel electrodes of graphene and single-wall carbon nanotube cogel. These cogel electrodes had large surface area (~800 m^2 g^{-1}) that enabled high enzyme loading, large porosity for unhindered glucose transport and moderate electrical conductivity (~0.2 S cm^{-1}) for efficient charge collection. Glucose oxidase and bilirubin oxidase were physically adsorbed onto these electrodes to form anodes and cathodes, respectively, and the EBFC produced power densities up to 0.19 mW cm^{-2} that correlated to 0.65 mW mL^{-1} or 140 mW g^{-1} of GOX with an open circuit voltage of 0.61 V. Further, the electrodes were rejuvenated by a simple wash and reloading procedure. We postulate these porous and ultrahigh surface area electrodes will be useful for biosensing applications, and will allow reuse of EBFCs.

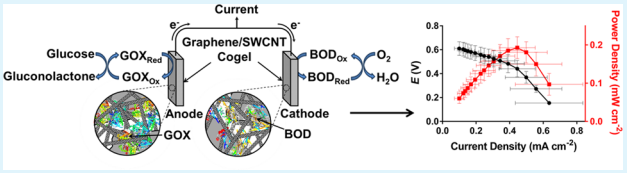

KEYWORDS: *biofuel cell, aerogel, glucose, enzymes, graphene, single-walled carbon nanotubes*

INTRODUCTION

The prospect of sustainable energy generation from readily available and renewable biofuels through the use of enzymatic biofuel cells (EBFCs) has been the target of significant research in recent years.[1−5] EBFCs utilize enzymes to convert the chemical energy in fuels such as glucose,[6−8] fructose[9−11] or alcohols[12−14] into electrical power via oxidation of fuel at the anode and reduction of an oxidant (typically molecular oxygen) at the cathode. The mild operation conditions and inherent biocompatibility of the enzyme-based system, along with the high specificity of enzymes, leading to membrane-less systems and thus an ease of miniaturization, make EBFCs ideal candidates for the continuous powering of implantable devices.[15−17] However, EBFCs currently suffer several key limitations including limited power output, instability over time and lack of reusability, which must be overcome to make their utilization a reality.

The low power output and short lifetime of EBFCs stems from multiple factors, with the main contributors being poor electron transfer from enzyme active site to electrode, and low levels of active enzyme loading onto the electrodes. Attempts to solve these issues have been focused on improvements to electrode materials and enzyme immobilization strategies. As the redox active sites of many enzymes are buried deeply within the three-dimensional protein shell, it is difficult to establish direct electron transfer (DET) to the electrode.[18,19] For example, the flavin adenine dinucleotide (FAD) cofactor of glucose oxidase (GOX), the most commonly studied anodic enzyme, is located roughly 15 Å below the protein surface, resulting in a large electron transfer resistance.[20] There have been two broadly investigated methods aimed at improving electron transfer efficiency. First, small molecules have been used as mediators (i.e., osmium or ferrocene containing complexes, 2,2′-azino-bis(3-ethylbenzthiazoline)-6-sulfonic

Received: November 7, 2014
Accepted: February 2, 2015
Published: February 2, 2015

DOI: 10.1021/am507801x
ACS Appl. Mater. Interfaces 2015, 7, 4056−4065

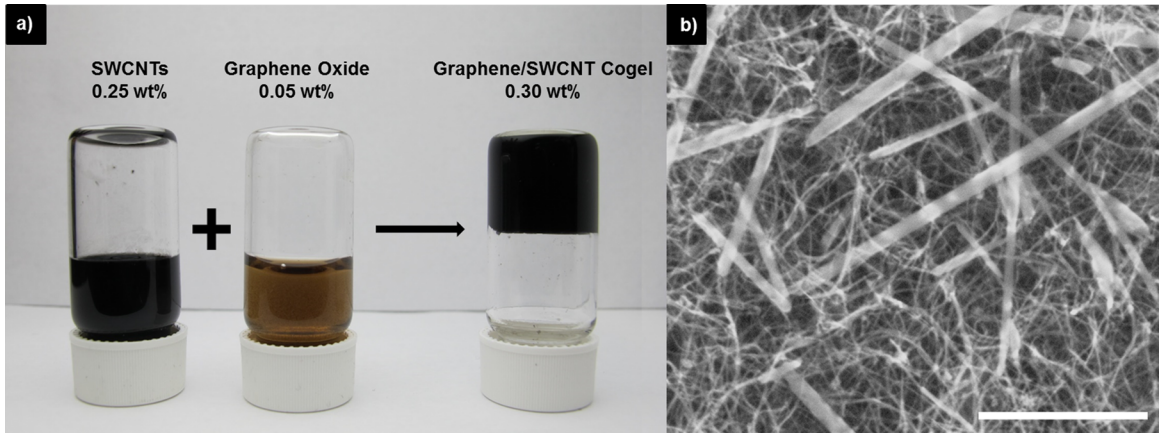

Figure 1. Graphene/SWCNT cogel. (a) Graphene/SWCNT cogel was formed by mixing individually dispersed SWCNTs with graphene oxide in a 5:1 ratio by weight. (b) Scanning electron microscopy (SEM) micrograph of graphene/SWCNT aerogel with scale bar representing 5 μm.

acid, etc.)[7,21−25] that serve to mediate electron transfer from active site to electrode. Second, electrode materials that have large surface area and are capable of close communication with the enzyme active site, such as carbon nanotubes, graphene or metal nanoparticles, have been utilized to increase enzyme loading and enhance electron transfer from enzyme to electrode.[6−8,26]

Mediated electron transfer (MET) type systems have been proven to possess enhanced electron transport capabilities and thus higher power outputs compared to identical setups without mediators, but also have several drawbacks.[24,27,28] For MET to be feasible, the redox potentials of the mediators must lay within the bounds of the anodic and cathodic enzyme prosthetic site redox potentials, thus reducing the maximum theoretical open-circuit voltage (OCV) of the overall system. Additionally, the leakage and instability of mediator groups adds toxicity and further power instability concerns for the EBFC, respectively. For instance, a naphthoquinone mediator has been shown to increase EBFC power output by 23% compared to an identical EBFC without a mediator. However, power stability and OCV of the mediated system markedly decreased to 40% power retained after 7 days and 0.76 V, respectively, compared to 96% power retained after 30 days and 0.95 V in the nonmediated system.[6,27] The presence of free mediator, by design or by leaching from the electrode due to their low molecular weight, can also increase potentially harmful effects in vivo and necessitate the use of a membrane to separate anodic and cathodic compartments, which adds to system complexity.[7] Thus, there exists a large drive to develop improved EBFCs with increased power densities utilizing materials capable of promoting electron transfer without the need for these types of externally added redox mediators.[4,18] In this report, we define systems operating without the addition of external redox mediators as "mediator-free".

Nanostructured materials such as nanotubes[26,29] and nanoparticles[30−32] are well suited to enhance current densities.[33−35] Carbon nanotubes (CNTs) are particularly good materials for this purpose because of their high electrical conductivity, nanometer scale dimensions, electrochemical stability and high aspect ratios.[6,35] Nevertheless, many configurations utilizing CNTs still require the use of mediators to achieve optimal performance and there is much debate over whether CNT-based systems are truly capable of achieving DET with FAD containing enzymes such as GOX.[7,19,24,36] However, CNT-based or CNT decorated systems still boast some of the highest reported power densities to date[7,24,27,37] even without the use of mediators.[6] Power densities of mediator-free, CNT-based EBFCs have reached up to 1.25 mW cm^{-2}, which corresponded to 1.66 mW mL^{-1} and 33 mW g^{-1} of GOX, for a system composed of compressed disks of multiwall CNTs and enzymes.[6] The electron transfer rate constant (k_s), which is a key measure of electron transfer efficiency, in systems using GOX immobilized on CNTs has been shown to reach up to 13 s^{-1}.[7] Graphene has also attracted significant interest as an electrode material for enzyme-based systems due to its excellent thermal and electrical conductivity, good biocompatibility and high specific surface area.[7,38,39] CNTs, graphene and other nanomaterials can further be manipulated to form three-dimensional, porous structures that allow for high enzyme loading and connectivity with an ease of substrate diffusion into the network.[6,8] Incorporation of large amounts of enzyme within such a network serves to surround the enzyme with conductive material to reduce the loss of electrons to outside electron acceptors (i.e., molecular oxygen) and potentially reduce the leaching of enzyme during operation. Previous reports have investigated such three-dimensional systems; however, most have exhibited reduced available surface area and enzyme activity after fabrication[6] or required the use of external mediators.[7,8,27] Unfortunately, due to the fabrication process and porosity, these electrodes cannot simply be reused by replacing degraded enzymes with fresh, active enzymes.

Herein, we report on the development of the first glucose-based, mediator-free EBFC utilizing free standing cogels of graphene and single-wall carbon nanotubes (SWCNT) as electrodes (Supplementary Figure S1). The graphene/SWCNT cogels were fabricated by mixing suspensions of graphene oxide and individually dispersed SWCNTs at suitable concentrations that led to percolating networks of interspersed graphene and SWCNTs (Figure 1). These gels possessed high specific surface area (SSA), porosity, and electrical conductivity that allowed high enzyme loading, unhindered glucose transport to the enzymes and efficient charge collection from enzymes. GOX from *Aspergillus niger* was used as the anodic enzyme of interest and the multicopper oxidase bilirubin oxidase (BOD) from *Myrothecium sp.* was the cathodic enzyme. We further determined the electrochemical characteristics of both anode and cathode individually as well as the simple, membrane- and mediator-free full cell. Finally, we examined reusability of the

DOI: 10.1021/am507801x
ACS Appl. Mater. Interfaces 2015, 7, 4056−4065

electrodes by washing away degraded enzymes and then reloading the electrodes with fresh, active enzymes.

MATERIALS AND METHODS

Materials. Ultrapure Milli-Q grade water (resistivity of 18.2 MΩ cm) was used for all experiments. Single-wall carbon nanotubes (SWCNTs) batch CG 200 with average diameter of 1 nm and average length of 1 μm were purchased from Southwest Nanotechnologies Inc. Graphite flakes were procured from Bay Carbon Inc. GOX from *Aspergillus niger* (100−250 units mg^{-1}), hydrogen peroxide and horseradish peroxidase were purchased from Sigma-Aldrich. BOD from *Myrothecium spagyrica* (2.7 units mg^{-1}) was purchased from Amano Enzyme Inc. All chemicals were of analytical grade and used as received. Sodium phosphate (NaPhos) buffer (0.1 M, pH 7.0), used for preparation of enzyme solutions and testing of electrodes, was prepared from phosphate salts.

Equipment. Sonication and centrifugation of nanotube solutions were carried out using a Thermo Fisher 500 probe tip sonicator and a Beckman Coulter L-100K ultracentrifuge, respectively. Adsorption spectra of SWCNT solutions were measured using a Varian Cary 5000 UV−visible NIR spectrophotometer. Critical point drying of ethanol saturated gels was performed on an Autosamdri 815 critical point dryer (Tousimis Research Corporation). Aerogel surface area was measured through nitrogen adsorption and desorption at 77 K using a Gemini VII 2390 surface area analyzer (Micromeritics) using the Brunauer−Emmett−Teller (BET) theory.[40] Pore volume and pore size distribution were calculated from the measured desorption isotherms using the Barret−Joyner−Halenda (BJH) calculation scheme. The characteristic morphologies of the aerogels were imaged using scanning electron microscopy (SEM, FEI Quanta 600) at 10 kV. Electrical conductivities of the gels were measured by two-probe contact direct current measurements using a Fluke 287 True RMS multimeter.

All electrochemical measurements were performed using a conventional three-electrode electrochemical cell utilizing a KCl saturated Ag/AgCl electrode and a 0.5 mm platinum wire electrode as reference and counter electrodes, respectively, and the gel electrode under study was used as the working electrode. Biofuel cell performance was monitored using a Fluke 287 True RMS multimeter with an IET Labs RS-200 resistance decade box that was used to manually vary EBFC resistance. GOX kinetic analysis was performed using the standard GOX 2,2′-azino-bis(3-ethylbenzthiazoline)-6-sulfonic acid (ABTS) activity assay at varying glucose concentrations, monitoring change in absorbance at 415 nm.

Fabrication of Graphene/SWCNT Cogels. SWCNT dispersions were prepared as previously described.[41−44] Briefly, we first sonicated SWCNTs in sodium dodecylbenzenesulfonate (SDBS) solution (1.0 wt %) at a SWCNT:SDBS ratio of 1:10 at 60 W for 2 h and removed aggregates through centrifugation for 15 min at 35000 rpm. We then determined the concentration of dispersed SWCNTs through UV−vis spectroscopy using an extinction coefficient of 2.6 absorbance mL mg^{-1} mm^{-1}[41] at 901 nm and the Beer−Lambert law. We synthesized graphene oxide via a modified Hummers' method.[45,46] The graphene oxide was then thoroughly washed by multiple water rinse and centrifugation steps. Subsequently, we added graphene oxide to dispersed SWCNT suspension at a graphene oxide:SWCNT ratio of 1:5, briefly sonicated to mix and concentrated to ∼0.3 wt % carbon-based materials via slow water evaporation at 60 °C. To form the desired shape, we degassed and pipetted the solution into the 2 mm thick rectangular molds. The mixed suspension of graphene oxide and SWCNTs gelled within a few minutes to a couple of hours. We allowed these graphene oxide/SWCNT cogels to age for roughly 12 h to improve their mechanical integrity. We removed the SDBS surfactant from the cogels by repeated washing with ultrapure water and one washing with nitric acid (1 M) for 20 min followed by thorough washing with ultrapure water to neutralize acid within the cogels. The graphene oxide was then converted to graphene by hydrothermal reduction of graphene oxide/SWCNT cogels at 185 °C for 18 h. Finally, water was exchanged with ethanol at increasing ethanol concentrations up to 100% and the cogels were transformed into aerogels via critical point drying. We further reduced graphene using pyrolysis at 900 °C for 6 h to yield the final graphene/SWCNT aerogels. The fabrication process of graphene/SWCNT cogels and aerogels is summarized in Figure 1. We refer to an interspersed network of graphene and SWCNT in any liquid as a cogel and in air as an aerogel. All graphene/SWCNT cogel-based electrodes used in this study had a cross-sectional area of ∼0.3 cm^2 and were ∼0.2 cm thick.

Preparation and Test of Biofuel Cells. To load enzymes into the electrodes, we incubated individual graphene/SWCNT aerogels in 2 mL of enzyme (GOX or BOD) solution (1 mg mL^{-1} in NaPhos buffer (0.1 M, pH 7.0)) for 4 h at 4 °C. To induce complete loading of these electrodes with enzyme solution, without collapsing the cogels, we applied a weak pulsed vacuum for several minutes using a benchtop vacuum pump prior to incubation. We then individually washed each enzyme-loaded cogel in 5 mL of NaPhos buffer (0.1 M, pH 7.0) for 10 min to remove any weakly bound enzymes. Finally, we carried out EBFC measurements in air saturated 200 mL NaPhos buffer (0.1 M, pH 7.0) solution with 100 mM glucose under stirring with enzyme-loaded cogel electrodes securely attached to wire leads via copper clips that were minimally exposed to buffer solution. Reloading of fuel cell electrodes was carried out after 20 min incubation in nitric acid (1 M) and thorough washing with ultrapure water.

RESULTS AND DISCUSSION

Material Characterization. We have previously shown that suspensions of SWCNTs can undergo sol−gel transition to form robust, three-dimensional networks owing to van der Waals forces acting between individually dispersed nanotubes.[41−43,47,48] Aerogels of CG 200 SWCNTs prepared via this process typically have electrical conductivities of $\kappa \sim 1$ S cm^{-1} and high SSA of ∼1290 m^2 g^{-1}, making them highly attractive as EBFC electrodes.[41] We note that the aerogel fabrication process, including acid treatment, has been previously shown not to damage the electrical transport properties of the nanotubes.[41] However, the majority of pores within the reported SWCNT gels had diameters of ∼2−8 nm, which was too small for efficient internalization of globular proteins such as GOX (8 × 7 × 8 nm).[41,49] A network of micrometer-sized graphene sheets and SWCNTs would likely possess larger pores throughout the matrix and enhance globular protein internalization.

Consequently, we fabricated free-standing, three-dimensional graphene/SWCNT cogels (Figure 1) having a density of 7.1 mg mL^{-1} and examined their pore/surface area characteristics and morphologies via BET and SEM, respectively (Figure S2 (Supporting Information) and Figure 1b). As expected, more than 70% of total pore volume in these the graphene/SWCNT cogels was made up of pores having a radius greater than 10 nm, as calculated from BET surface area measurements according to the BJH calculation scheme (Figure S2, Supporting Information), meaning a large majority of the electrode was potentially accessible to the diffusion of electroactive enzymes. The micron scale graphene sheets, which form scroll-like structures[50] within the SWCNT matrix, were easily discernible in SEM images (Figure 1b) from the nanosized SWCNTs. The final graphene/SWCNT aerogels possessed moderate electrical conductivity (κ = 0.2 S cm^{-1}) and ultrahigh surface area (SSA = 846 m^2 g^{-1}), and were further functionalized via physical adsorption of GOX or BOD to form EBFC anodes or cathodes, respectively.

Characterization of the GOX-based Anode. The GOX-catalyzed degradation of glucose proceeds as follows

$$GOX_{FAD} + \text{glucose} \rightarrow GOX_{FADH_2} + \text{gluconolactone} \quad (1)$$

DOI: 10.1021/am507801x
ACS Appl. Mater. Interfaces 2015, 7, 4056−4065

$$GOX_{FADH_2} \rightarrow GOX_{FAD} + 2H^+ + 2e^- \quad (2)$$

Upon GOX functionalization, we electrochemically characterized the cogel anodes in order to evaluate their performance. OCV evolutions of the cogel with and without immobilized GOX were examined to determine electron transfer between enzyme and electrode (Figure 2). The OCV of the modified anode in the presence of 10 mM glucose was −0.05 ± 0.01 V versus Ag/AgCl. The thermodynamically determined redox potential of the $FAD/FADH_2$ couple of GOX has been shown to be approximately −0.36 V versus Ag/AgCl.[51] The overpotential between the thermodynamically determined and experimentally observed potentials may have been caused by decreases in native enzyme activity due to partial denaturation upon physical adsorption or the blockage of electrically connected FAD sites to glucose binding.[52,53] Nevertheless, the observed decrease in OCV upon anode functionalization indicated successful adsorption of enzyme and electron transfer between active site and electrode.

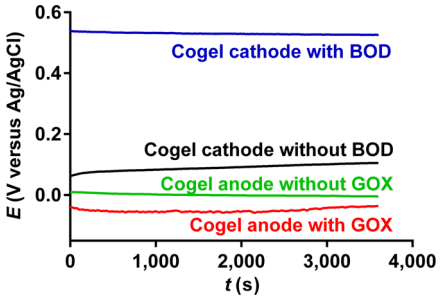

Figure 2. Open circuit voltages of graphene/SWCNT cogel-based anode and cathode. Open circuit voltage evolution of cathode with and without BOD, and anode with and without GOX in NaPhos buffer (0.1 M, pH 7.0) containing substrate. Anodic measurements carried out with 10 mM glucose and cathodic measurements with O_2 saturated solution.

Cyclic voltammetry (CV) measurements of the GOX functionalized graphene/SWCNT cogel electrodes showed obvious oxidation and reduction peaks at −0.34 and −0.51 V, respectively, indicating quasi-reversible electron transfer between FAD groups and the anode surface (Figure 3a). Additionally, the current response increased slightly upon the addition of glucose into the system, indicative of some level of GOX activity. This further confirmed the successful incorporation of GOX into the gel network as the discussed faradaic current response was absent in CV scans of bare graphene/SWCNT gels (Figure 3a) and no current shifts were observed upon the addition of glucose to nonfunctionalized systems (Figure S3, Supporting Information).

However, these results alone do not sufficiently prove that we observed DET of enzymatically active GOX. Stevenson et al. recently reported significant evidence that DET with enzymatically active GOX at CNTs is not possible and that electrochemical responses observed in DET claiming studies were a result of free FAD immobilized onto CNT surfaces.[19] This conclusion was also reached by Ye et al. concerning graphene surfaces.[36] Stevenson et al. also suggested that the appearance of anodic current upon glucose addition is likely the most appropriate signature of DET with an FAD-containing enzyme such as GOX.[19] To study the potential DET of GOX immobilized onto graphene/SWCNT cogels in depth, we performed amperometry along with additional CV traces (Figure S4, Supporting Information). We observed a slow anodic shift in current upon the addition of glucose to GOX-functionalized graphene/SWCNT cogels in Ar saturated solution (Figure S4a, Supporting Information) and in O_2 saturated solution (Figure S4b, Supporting Information) with

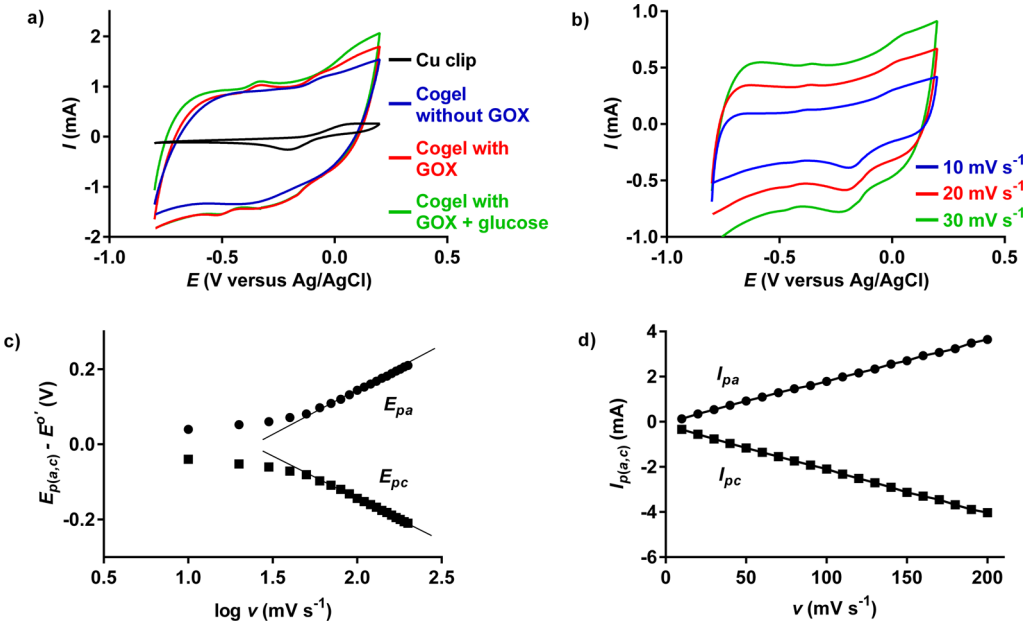

Figure 3. Electrochemical performance of graphene/SWCNT cogel-based anode. (a) CV traces of bare copper clip, graphene/SWCNT cogel anode, GOX functionalized graphene/SWCNT anode and GOX functionalized graphene/SWCNT anode in 10 mM glucose at 50 mV s^{-1}. (b) CV traces of GOX functionalized graphene/SWCNT anode at varying scan rates between 10 mV s^{-1} to 30 mV s^{-1}). (c) Dependence of anodic (circle) and cathodic (square) peak potentials on the logarithm of scan rate for GOX functionalized graphene/SWCNT anode at varying scan rates. (d) Dependence of anodic (circle) and cathodic (square) peak currents on scan rate for GOX functionalized graphene/SWCNT anode at varying scan rates. Experiments carried out in Ar saturated NaPhos buffer (0.1 M, pH 7.0).

DOI: 10.1021/am507801x
ACS Appl. Mater. Interfaces 2015, 7, 4056−4065

voltage held at the observed formal potential (−0.42 V). The appearance of this shift in Ar saturated solution suggested DET of GOX. We further examined the response of GOX functionalized electrodes to glucose addition by measuring CV characteristics at a scan rate of 5 mV s^{-1}. In both Ar and O_2 saturated solutions, anodic current increased, which was indicative of current generated through the oxidation of glucose by electrically connected GOX (Figure S4c,d, Supporting Information). Also, we noted a significant decrease in the cathodic peak current in O_2 saturated solution, which we attributed to a decrease in O_2 concentration due to the enzymatic reduction of O_2 to hydrogen peroxide (Figure S4d, Supporting Information). To ensure this cathodic peak and amperometric shift were not caused by O_2 reduction at the electrode surface uncoupled from GOX kinetics, we performed CV traces of nonfunctionalized graphene/SWCNT cogels in both Ar and O_2 saturated solutions and saw no change (Figure S4e, Supporting Information). From these results, we postulate that DET between GOX and graphene/SWCNT cogels was observed and, independent of these findings, we define the system to be mediator-free, as no external redox mediators were added at any point.

We further investigated the electron transfer between immobilized GOX/FAD and graphene/SWCNT cogel electrodes by measuring the CV characteristics of the anode at varying scan rates (Figure 3b). The dependence of anodic and cathodic peak potentials on the logarithm of scan rates from 10 to 100 mV s^{-1} was examined (Figure 3c) and used to determine anodic electrochemical parameters according to eqs 3 and 4.[54,55]

$$E_{pc} = E'^{\circ} - \left[\frac{RT}{\alpha nF}\right]\ln\left[\frac{\alpha Fn}{RTk_s}v\right] \tag{3}$$

$$E_{pa} = E'^{\circ} + \left[\frac{RT}{(1-\alpha)nF}\right]\ln\left[\frac{(1-\alpha)Fn}{RTk_s}v\right] \tag{4}$$

In eqs 3 and 4, E'° is the formal potential of the system equal to the average of anodic and cathodic peak potentials, α designates the charge transfer coefficient of the system, v is the scan rate used, n is the number of electrons transferred in the reaction, k_s is the heterogeneous electron transfer rate constant and T, R and F are temperature, the ideal gas constant and Faraday's constant, respectively. Based on these equations, n and α were calculated from the slopes of the lines from the linear region at high scan rates (Figure 3c). Specifically, the trend lines passing through these points gave straight lines whose slopes were equivalent to $-2.3RT/[\alpha nF]$ for the cathodic peaks and $2.3RT/[(1-\alpha)nF]$ for the anodic peaks (eqs 3 and 4).[54] Thus, α and n were found to be 0.5 and 0.54, respectively. The calculated α value was similar to other studies reported.[26,56] however, the value of n was markedly lower than the theoretical value for the conversion of FAD to $FADH_2$ in GOX, suggesting potentially hindered electron transport. Additionally, the k_s of the system was calculated using eq 5.[54]

$$\log k_s = \alpha\log(1-\alpha) + (1-\alpha)\log\alpha - \log\left(\frac{RT}{nFv}\right) - \alpha(1-\alpha)\left(\frac{nF\Delta E_p}{2.3RT}\right) \tag{5}$$

From eq 5, the k_s of the graphene/SWCNT-based system was estimated to be 0.23 ± 0.01 s^{-1}, which was slightly lower than similar reports[56−58] due to the larger separation of peak potentials.

As can be seen in Figure 3d, the anodic and cathodic peak currents of the GOX functionalized graphene/SWCNT cogel increased linearly with scan rate. This result implied that the system was limited by the electron transfer occurring at the enzyme−electrode interface rather than by diffusion of glucose through the porous network. Further, we used the slopes of these lines to estimate the loading of electroactive species on the surface of the electrode according to eq 6.[59]

$$i_p = \frac{n^2F^2\Gamma A}{4RT}v \tag{6}$$

In eq 6, Γ signifies the surface coverage of electroactive species (i.e., FAD sites),[57] A is the surface area available for adsorption of the electroactive species and i_p is the peak current. The estimated specific surface area coverage of FAD/$FADH_2$ was 1.44×10^{-12} mol cm^{-2} or 1.73×10^{-8} mol cm^{-2} of cross-sectional area, indicating the efficient internalization of GOX into the cogel matrix, resulting in high loadings. Assuming an average diameter of 8 nm for each GOX molecule, the calculated loading corresponded to more than 20% of available cogel surface area being occupied by electroactive GOX presuming two molecules of FAD indicated one GOX molecule. This loading was almost 2 orders of magnitude higher than similar three-dimensional structures comprised of Pd aerogels[8] or graphene foams decorated with SWCNTs.[7] Using the apparent concentration of immobilized GOX, we determined the retained enzyme kinetics upon immobilization. Specifically, the catalytic rate constant (k_{cat}) of immobilized GOX was 46 ± 3 s^{-1} compared to 316 ± 16 s^{-1} for native enzyme (Figure S5, Supporting Information). This decrease is common for immobilized enzymes due to partial denaturation at the enzyme-nanosupport interface upon attachment.[53] Despite the reduction of catalytic efficiency, k_{cat} was greater than the observed k_s, suggesting an electron transport-limited system.

Characterization of the BOD-based Cathode. BOD is a multicopper oxidase that serves to accept electrons from the electrode at the T1 copper site and transfer those electrons approximately 13 Å to the T2/T3 copper site where oxygen is reduced to water in a four-electron transfer mechanism according to eq 7.[60,61]

$$O_2 + 4H^+ + 4e^- \rightarrow 2H_2O \tag{7}$$

As can be seen in Figure 2, the OCV of the BOD-functionalized cathode was 0.53 ± 0.01 V versus Ag/AgCl, which was in agreement with reported OCVs in similar studies.[62] This value was slightly more positive than the thermodynamically determined value of the T1 copper site of BOD, which has been reported to be approximately 0.47 V versus Ag/AgCl.[63] The observed increase in OCV compared to bare graphene/SWCNT cogels at similar conditions confirmed the presence of immobilized BOD and, more importantly, showed the efficient electron transfer between enzyme active site and electrode. Lower overpotentials were likely achieved for BOD compared to GOX due to the closer proximity of the T1 electron acceptor site to the surface of BOD relative to the FAD active site of GOX.[61]

DOI: 10.1021/am507801x
ACS Appl. Mater. Interfaces 2015, 7, 4056−4065

To further confirm the presence of electrically connected enzyme on the cathode, we examined BOD-functionalized and nonfunctionalized electrodes using CV. CV sweeps did not yield any redox transformation evident by the lack of faradaic current response (Figure 4), which was consistent with

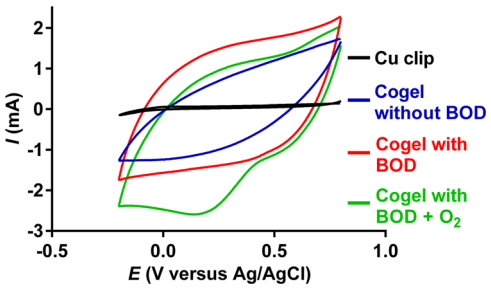

Figure 4. Electrochemical performance of graphene/SWCNT cogel-based cathode. CV traces of bare copper clip, graphene-SWCNT cogel cathode, BOD functionalized graphene/SWCNT cathode in Ar saturated solution and BOD functionalized graphene/SWCNT cathode in O_2 saturated solution at 50 mV s^{-1}. Experiments carried out in NaPhos buffer (0.1 M, pH 7.0).

previous reports on the electrochemical activity of BOD[64] and other multicopper oxidases.[65] However, upon addition of O_2 to the BOD functionalized system a significant decrease in cathodic current was observed with an onset potential of oxygen reduction of ~0.4 V versus Ag/AgCl. This result showed the capability of immobilized BOD to achieve DET and efficiently reduce oxygen to water.[8,66,67] We stress that no response to the addition of O_2 occurred in our system without the presence of BOD (Figure S6, Supporting Information), showing that the immobilized enzyme was solely responsible for O_2 reduction.

EBFC Performance. We set up EBFCs using a single GOX-loaded graphene/SWCNT cogel anode and a single BOD-loaded graphene/SWCNT cogel cathode (Figure S1, Supporting Information), and tested power output through the manual variation of circuit resistance while measuring voltage output. The performance of an EBFC can be expressed through the use of two main characteristics: OCV and power density. For our mediator-free graphene/SWCNT-based system, the OCV was 0.61 ± 0.05 V and the cross-sectional power density was 0.19 ± 0.03 mW cm^{-2} operating at 0.44 V (Figure 5).

This power output corresponded to 0.08% of native GOX activity relative to GOX turning over glucose at the

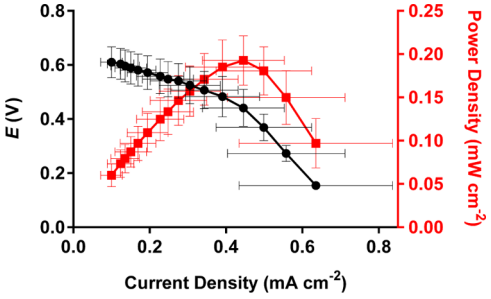

Figure 5. Performance of graphene/SWCNT cogel-based EBFC. Graphene/SWCNT cogel-based EBFC performance and cell polarization curves. Experiments carried out in air saturated NaPhos buffer (0.1 M, pH 7.0) with 100 mM glucose. Error bars represent standard deviation of three trials.

experimentally determined k_{cat} of native enzyme and GOX loading. In other words, we found the experimental power density to have an efficiency of 0.08% of the maximum, corresponding to the calculated amount of GOX per unit area generating current from glucose at the reported k_{cat} of native GOX. The observed percentage activity was in agreement with similar EBFC systems.[6] The experimental full-cell OCV was in good agreement with the difference between OCVs of the individual anode and cathode (i.e., −0.05 and 0.53 V versus Ag/AgCl, respectively) as expected. The polarization curve showed the maximum power output corresponded to a current density which was lower than the onset of concentration losses caused by limited diffusion of reactants and products (i.e., increased negative slope at high current density)[1] (Figure 5). Further, the operation of the EBFC was tested at pH 5.5 for optimal GOX activity (Figure S7, Supporting Information), but yielded essentially no change from the EBFC performance at pH 7. This result confirmed that the overall system was limited by electron transfer at the anode and not intrinsic enzyme activity. We further tested if the oxidation of glucose by GOX generated the current in the system through a series of control experiments without GOX. First, we immersed the copper leads alone in the EBFC solution with no graphene/SWCNT cogels or enzyme and tested for current generation. Then, we examined the performance of EBFCs with bare graphene/SWCNT cogels without any adsorbed enzyme as an anode and a cathode, followed by tests using a bare cogel as the anode and a cogel loaded with BOD as the cathode. The resulting performance and polarization curves exhibited negligible current generation (Figure S8, Supporting Information), which confirmed a GOX-driven system. Additionally, an interesting question that has never been addressed for EBFCs was whether the electrodes can be reloaded when the enzymes degrade. The robustness and simple loading procedure of our system allowed us to clean and then "refill" the electrodes with active enzymes. Rejuvenation of power output by cyclic removal of degraded enzyme with acid and replenishing the system with fresh, active enzyme generated a power density of 0.15 ± 0.02 mW cm^{-2} (Figure 6).

Conventionally, the power densities of fuel cells have been reported in cm^{-2} as the flow of current is a flux through the electrode surface. Most reported EBFC systems are essentially two-dimensional, such as functionalized coatings on pre-existing material surfaces (i.e., glassy carbon electrodes

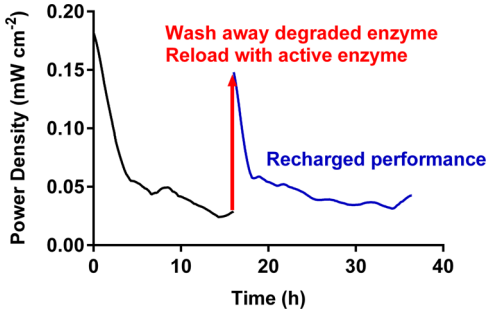

Figure 6. Continuous performance and recharging of graphene/SWCNT cogel-based EBFC. Performance of graphene/SWCNT cogel-based EBFC over time. Acid washing of degraded enzyme and reloading with active enzyme after 18 h followed by (blue) repeated performance. Experiments carried out in air saturated NaPhos buffer (0.1 M, pH 7.0) with 100 mM glucose.

DOI: 10.1021/am507801x
ACS Appl. Mater. Interfaces 2015, 7, 4056−4065

Table 1. Performance of Published Glucose-Driven EBFC Systems Utilizing Graphene or Carbon Nanotube-based Electrode Materials[a]

anode	cathode	mediator-free/MET (membrane Y/N)	OCV (V)	power density	reference
GOX-graphene/SWCNT cogel	BOD-graphene/SWCNT cogel	mediator-free (N)	0.61	0.19 mW cm^{-2} 0.65 mW mL^{-1}	this work
GOX/catalase-compressed MWCNT disk	laccase-compressed MWCNT disk	mediator-free (N)	0.57	0.19 mW cm^{2} 0.16 mW mL^{-1}	ref 17
PQQ-GDH-PANi/MWCNT modified Au electrode	BOD-MWCNT modified gold electrode	mediator-free (N)	0.68	0.07 mW cm^{-2}	ref 72
GOX-SWCNT/PPY 3D composite	tyrosinase-CNP/PPY composite	mediator-free (N)	0.19	0.16 mW mL^{-1}	ref 73
GOX/catalase-compressed MWCNT disk	laccase-compressed MWCNT disk	mediator-free (Y)	0.95	1.25 mW cm^{-2} 1.66 mW mL^{-1}	ref 6
cross-linked GOX clusters-MWCNT/Nafion	Pt/C/Nafion	mediator-free (Y)	0.43	0.18 mW cm^{-2}	ref 70
GOX/Fc-Pd aerogel	BOD-Pd/Pt aerogel	MET (N)	0.40	0.02 mW cm^{-2}	ref 8
Nafion/GOX/Fc-3D graphene network/GCE	Nafion/laccase-3D graphene network/PTCA/DA/GCE	MET (N)	0.40	0.11 mW cm^{-2}	ref 39
(MWCNT/thionine/AuNPs) GDH	MWCNT/PLL/laccase	MET (N)	0.70	0.33 mW cm^{-2}	ref 75
vaCNT/PABMSA/PQQ-GDH	vaCNT/PQQ/BOD	MET (N)	0.80	0.12 mW cm^{-2}	ref 76
PPY/SWCNT/GOX	PPY/laccase/ABTS	MET (N)	0.77	1.39 mW cm^{-2} 232 mW mL^{-1}	ref 24
GOX/PEDOT/MWCNT/PVI−Os/PEGDGE	BOD/PEDOT/MWCNT/PAA−PVI-Os/PEGDGE	MET (N)	0.70	2.18 mW cm^{-2} 793 mW mL^{-1}	ref 74
GOX-graphene/SWCNT foam	laccase/ABTS-graphene/SWCNT foam	MET (Y)	1.2	2.27 mW cm^{-2}	ref 7
GOX/catalase/NQ-compressed MWCNT disk	laccase-compressed MWCNT disk	MET (Y)	0.76	1.54 mW cm^{-2} 1.92 mW mL^{-1}	ref 27

[a]MET, mediated electron transfer; OCV, open circuit voltage; MWCNT, multiwall carbon nanotube; PQQ-GDH, pyrroloquinoline quinone dependent glucose dehydrogenase; PANi, polyaniline; PPY, polypyrrole; CNP, carbon nanopowder; Fc, ferrocenecarboxylic acid; PTCA, 3,4,9,10-perylene tetracarboxylic acid; DA, dopamine; AuNPs, gold nanoparticles; PLL, poly-L-lysine; vaCNT, vertically alighned carbon nanotube; PABMSA, poly(3-aminobenzoic acid-*co*-2-methoxyaniline-5-sulfonic acid; PEDOT, poly(3,4-dioxythiophene); PVI−Os, poly(*N*-vinylimidazole)-[Os(4,4′-dimethoxy-2,2′-bipyridine)$_2$Cl]$^{+/2+}$; PEGDGE, poly(ethylene glycol) diglycidyl ether; PAA−PVI-Os, poly(acrylamide)-poly(*N*-vinylimidazole)-[Os(4,4′-dichloro-2,2′-bipyridine)$_2$]$^{+/2+}$; ABTS, 2.2′azinobis(3-ethylbenzothiazoline-6-sulfonic acid) diammonium salt; NQ, naphthoquinone.

(GCE), buckeypaper, etc.).[25,68−70] Recently, however, EBFC systems utilizing three-dimensional electrodes have gained increased attention and resulted in enhanced power densities due to the possibility of increased active enzyme loadings and connectivity.[6,7,24,27,71] Thus, the need to report power densities volumetrically has arisen to allow for meaningful comparisons between studies. The volumetric power density of this system utilizing ∼2 mm thick graphene/SWCNT cogel electrodes was 0.65 ± 0.22 mW mL^{-1}. Further, it was important to characterize the system in terms of gravimetric power density to show the power output per mass of catalyst. The loading density of GOX onto the graphene/SWCNT cogel anodes was estimated through CV analysis at varying scan rates[57] knowing each GOX molecule contains two FAD sites.[59] The gravimetric power density of this system was 140 ± 20 mW g^{-1} GOX, which is more than 4-fold greater than the elegant systems based on compressed disks of multiwall carbon nanotubes and enzymes.[6] This increase compared to the similar mediator-free system was attributed to the fabrication procedure and high porosity of our system, which allowed the majority of incorporated enzyme to have access to both the electrode surface for electron transfer and to freely diffusing substrate.

The membrane-and mediator-free EBFC we describe herein can be added to a small but growing literature on similar systems,[6,72,73] including a setup resulting in a nearly identical cross-sectional power density that was successfully implanted into rats.[17] Multiple other studies have been able to produce higher performing fuel cells but have also required mediated electron transfer and even setups with multiple compartments separated by a semipermeable membrane, adding complexity and additional toxicity concerns.[7,27,37] Further, other mediator-free systems have commonly required more complicated electrode functionalization steps prior to enzyme immobilization[72,73] or large amounts of bulk enzyme due to low enzyme activity retention.[6] Due to the porosity, high surface area and significant electrical conductivity of the electrode materials used herein, we have been able to achieve relatively high enzyme loadings and rapid charge collection without significant loss, which resulted in a significant power density despite hindered electron transport. High enzyme loadings are relative to reported studies that used similar three-dimensional nanomaterial networks and enzyme immobilization strategies.[7,8] A comparison of various relevant studies focused on glucose-driven EBFCs utilizing graphene or carbon nanotube-based electrode materials is presented in Table 1. The EBFC reported herein had a power output within 1 order of magnitude of the highest performing systems to date.[7,27,74] Our data showed that the anodic electron transfer rate constant was lower than other investigators have found,[7] leading to a clear path for further improvement in our EBFC.

CONCLUSIONS

We have developed and characterized a membrane- and mediator-free EBFC utilizing novel graphene/SWCNT cogel electrodes. The glucose/O_2-fueled system proved capable of producing a power density of 0.19 ± 0.03 mW cm^{-2}, 0.65 ± 0.22 mW mL^{-1} or 140 ± 20 mW g^{-1} GOX with an OCV of 0.61 ± 0.05 V without the addition of external redox mediators. Compared to previous studies, the EBFC we describe was a robust, high power output system despite significantly hindered anodic electron transfer. We attributed the performance to the high available surface area and porosity of the electrode material

DOI: 10.1021/am507801x
ACS Appl. Mater. Interfaces 2015, 7, 4056−4065

allowing for large loading of active enzymes relative to similar studies and ease of glucose diffusion through the cogel-based electrode. The nanoscale structure and high electrical conductivity of the cogels facilitated electron transfer to the electrode surface and charge collection through the electrode without any toxic redox mediators. The robustness of the cogels and our custom-designed loading procedure also allowed for the reloading and reuse of the EBFC. This study demonstrated the potential of such a system and highlighted areas of possible improvement for enhanced EBFC performance. Future work will focus on increasing electron transfer efficiency and long-term stability.

■ ASSOCIATED CONTENT

Supporting Information

Schematic representation of EBFC system, graphene/SWCNT cogel pore size distribution data, CV results of nonfunctionalized cogel systems, native and immobilized GOX kinetic data, and EBFC performance at pH 5.5. This material is available free of charge via the Internet at http://pubs.acs.org.

■ AUTHOR INFORMATION

Corresponding Authors

*M. F. Islam: Tel.: +1 412 268 8999. Fax: +1 412 268 7596. E-mail: mohammad@cmu.edu.

*A. J. Russell: Tel.: +1 413 330 2404. Fax: +1 412 268 5229. E-mail: alanrussell@cmu.edu.

Author Contributions

M.F.I. and A.J.R. initiated the project. A.S.C. designed and carried out experiments. Y.J.J., R.R.K. and S.M.G. assisted with experiments. M.F.I. and A.J.R. gave technical and conceptual advice. A.S.C., M.F.I. and A.J.R. wrote the paper. All authors read and commented on the manuscript.

Notes

The authors declare no competing financial interest.

■ ACKNOWLEDGMENTS

Financial support for this work was provided by National Science Foundation through grants CBET-1335417 (M.F.I.) and CBET-1066621 (A.J.R.) and Heinz Endowment through grant E0530 (A.J.R.).

■ REFERENCES

(1) Meredith, M. T.; Minteer, S. D. Biofuel Cells: Enhanced Enzymatic Bioelectrocatalysis. *Annu. Rev. Anal. Chem.* **2012**, *5*, 157−179.

(2) Ammam, M. Electrochemical and Electrophoretic Deposition of Enzymes: Principles, Differences and Application in Miniaturized Biosensor and Biofuel Cell Electrodes. *Biosens. Bioelectron.* **2014**, *58*, 121−131.

(3) Leech, D.; Kavanagh, P.; Schuhmann, W. Enzymatic Fuel Cells: Recent Progress. *Electrochim. Acta* **2012**, *84*, 223−234.

(4) de Poulpiquet, A.; Ciaccafava, A.; Lojou, E. New Trends in Enzyme Immobilization at Nanostructured Interfaces for Efficient Electrocatalysis in Biofuel Cells. *Electrochim. Acta* **2014**, *126*, 104−114.

(5) Minteer, S. D.; Liaw, B. Y.; Cooney, M. J. Enzyme-based Biofuel Cells. *Curr. Opin. Biotechnol.* **2007**, *18*, 228−234.

(6) Zebda, A.; Gondran, C.; Le Goff, A.; Holzinger, M.; Cinquin, P.; Cosnier, S. Mediatorless High-Power Glucose Biofuel Cells Based on Compressed Carbon Nanotube-Enzyme Electrodes. *Nat. Commun.* **2011**, *2*, 370.

(7) Prasad, K. P.; Chen, Y.; Chen, P. Three-Dimensional Graphene-Carbon Nanotube Hybrid for High-Performance Enzymatic Biofuel Cells. *ACS Appl. Mater. Interfaces* **2014**, *6*, 3387−3393.

(8) Wen, D.; Liu, W.; Herrmann, A. K.; Eychmuller, A. A Membraneless Glucose/O_2 Biofuel Cell Based on Pd Aerogels. *Chem.—Eur. J.* **2014**, *20*, 4380−4385.

(9) So, K.; Kawai, S.; Hamano, Y.; Kitazumi, Y.; Shirai, O.; Hibi, M.; Ogawa, J.; Kano, K. Improvement of a Direct Electron Transfer-Type Fructose/Dioxygen Biofuel Cell with a Substrate-Modified Biocathode. *Phys. Chem. Chem. Phys.* **2014**, *16*, 4823−4829.

(10) Wu, X. E.; Guo, Y. Z.; Chen, M. Y.; Chen, X. D. Fabrication of Flexible and Disposable Enzymatic Biofuel Cells. *Electrochim. Acta* **2013**, *98*, 20−24.

(11) Miyake, T.; Haneda, K.; Yoshino, S.; Nishizawa, M. Flexible, Layered Biofuel Cells. *Biosens. Bioelectron.* **2013**, *40*, 45−49.

(12) Das, M.; Barbora, L.; Das, P.; Goswami, P. Biofuel Cell for Generating Power from Methanol Substrate Using Alcohol Oxidase Bioanode and Air-Breathed Laccase Biocathode. *Biosens. Bioelectron.* **2014**, *59*, 184−191.

(13) Neto, S. A.; Suda, E. L.; Xu, S.; Meredith, M. T.; De Andrade, A. R.; Minteer, S. D. Direct Electron Transfer-Based Bioanodes for Ethanol Biofuel Cells Using PQQ-Dependent Alcohol and Aldehyde Dehydrogenases. *Electrochim. Acta* **2013**, *87*, 323−329.

(14) Arrocha, A. A.; Cano-Castillo, U.; Aguila, S. A.; Vazquez-Duhalt, R. Enzyme Orientation for Direct Electron Transfer in an Enzymatic Fuel Cell with Alcohol Oxidase and Laccase Electrodes. *Biosens. Bioelectron.* **2014**, *61*, 569−574.

(15) Cosnier, S.; Le Goff, A.; Holzinger, M. Towards Glucose Biofuel Cells Implanted in Human Body for Powering Artificial Organs: Review. *Electrochem. Commun.* **2014**, *38*, 19−23.

(16) Halamkova, L.; Halamek, J.; Bocharova, V.; Szczupak, A.; Alfonta, L.; Katz, E. Implanted Biofuel Cell Operating in a Living Snail. *J. Am. Chem. Soc.* **2012**, *134*, 5040−5043.

(17) Zebda, A.; Cosnier, S.; Alcaraz, J. P.; Holzinger, M.; Le Goff, A.; Gondran, C.; Boucher, F.; Giroud, F.; Gorgy, K.; Lamraoui, H.; Cinquin, P. Single Glucose Biofuel Cells Implanted in Rats Power Electronic Devices. *Sci. Rep.* **2013**, *3*, 1516.

(18) Falk, M.; Blum, Z.; Shleev, S. Direct Electron Transfer Based Enzymatic Fuel Cells. *Electrochim. Acta* **2012**, *82*, 191−202.

(19) Goran, J. M.; Mantilla, S. M.; Stevenson, K. J. Influence of Surface Adsorption on the Interfacial Electron Transfer of Flavin Adenine Dinucleotide and Glucose Oxidase at Carbon Nanotube and Nitrogen-Doped Carbon Nanotube Electrodes. *Anal. Chem.* **2013**, *85*, 1571−1581.

(20) Wohlfahrt, G.; Witt, S.; Hendle, J.; Schomburg, D.; Kalisz, H. M.; Hecht, H. J. 1.8 and 1.9 Angstrom Resolution Structures of the Penicillium Amagasakiense and Aspergillus Niger Glucose Oxidases as a Basis for Modelling Substrate Complexes. *Acta Crystallogr., Sect. D: Biol. Crystallogr.* **1999**, *55*, 969−977.

(21) Mao, F.; Mano, N.; Heller, A. Long Tethers Binding Redox Centers to Polymer Backbones Enhance Electron Transport in Enzyme "Wiring" Hydrogels. *J. Am. Chem. Soc.* **2003**, *125*, 4951−4957.

(22) Jenkins, P.; Tuurala, S.; Vaari, A.; Valkiainen, M.; Smolander, M.; Leech, D. A Mediated Glucose/Oxygen Enzymatic Fuel Cell Based on Printed Carbon Inks Containing Aldose Dehydrogenase and Laccase as Anode and Cathode. *Enzyme Microb. Technol.* **2012**, *50*, 181−187.

(23) Mano, N.; Mao, F.; Heller, A. Characteristics of a Miniature Compartment-Less Glucose-O_2 Biofuel Cell and Its Operation in a Living Plant. *J. Am. Chem. Soc.* **2003**, *125*, 6588−6594.

(24) Kim, J.; Yoo, K. H. Glucose Oxidase Nanotube-based Enzymatic Biofuel Cells with Improved Laccase Biocathodes. *Phys. Chem. Chem. Phys.* **2013**, *15*, 3510−3517.

(25) Bunte, C.; Hussein, L.; Urban, G. A. Performance of Non-compartmentalized Enzymatic Biofuel Cell Based on Buckypaper Cathode and Ferrocene-Containing Redox Polymer Anode. *J. Power Sources* **2014**, *247*, 579−586.

(26) Yu, Y. Y.; Chen, Z. G.; He, S. J.; Zhang, B. B.; Li, X. C.; Yao, M. C. Direct Electron Transfer of Glucose Oxidase and Biosensing for Glucose Based on PDDA-Capped Gold Nanoparticle Modified Graphene/Multi-walled Carbon Nanotubes Electrode. *Biosens. Bioelectron.* **2014**, *52*, 147−152.

DOI: 10.1021/am507801x
ACS Appl. Mater. Interfaces 2015, 7, 4056−4065

(27) Reuillard, B.; Le Goff, A.; Agnes, C.; Holzinger, M.; Zebda, A.; Gondran, C.; Elouarzaki, K.; Cosnier, S. High Power Enzymatic Biofuel Cell Based on Naphthoquinone-Mediated Oxidation of Glucose by Glucose Oxidase in a Carbon Nanotube 3d Matrix. *Phys. Chem. Chem. Phys.* **2013**, *15*, 4892−4896.
(28) Gao, F.; Viry, L.; Maugey, M.; Poulin, P.; Mano, N. Engineering Hybrid Nanotube Wires for High-Power Biofuel Cells. *Nat. Commun.* **2010**, *1*, 2.
(29) Deng, C. Y.; Chen, J. H.; Nie, Z.; Si, S. H. A Sensitive and Stable Biosensor Based on the Direct Electrochemistry of Glucose Oxidase Assembled Layer-by-Layer at the Multiwall Carbon Nanotube-Modified Electrode. *Biosens. Bioelectron.* **2010**, *26*, 213−219.
(30) Patil, D.; Dung, N. Q.; Jung, H.; Ahn, S. Y.; Jang, D. M.; Kim, D. Enzymatic Glucose Biosensor Based on CeO_2 Nanorods Synthesized by Non-Isothermal Precipitation. *Biosens. Bioelectron.* **2012**, *31*, 176−181.
(31) Zhao, S.; Zhang, K.; Bai, Y.; Yang, W. W.; Sun, C. Q. Glucose Oxidase/Colloidal Gold Nanoparticles Immobilized in Nafion Film on Glassy Carbon Electrode: Direct Electron Transfer and Electrocatalysis. *Bioelectrochemistry* **2006**, *69*, 158−163.
(32) Holzinger, M.; Le Goff, A.; Cosnier, S. Carbon Nanotube/Enzyme Biofuel Cells. *Electrochim. Acta* **2012**, *82*, 179−190.
(33) Wooten, M.; Karra, S.; Zhang, M. G.; Gorski, W. On the Direct Electron Transfer, Sensing, and Enzyme Activity in the Glucose Oxidase/Carbon Nanotubes System. *Anal. Chem.* **2014**, *86*, 752−757.
(34) Minteer, S. D.; Atanassov, P.; Luckarift, H. R.; Johnson, G. R. New Materials for Biological Fuel Cells. *Mater. Today* **2012**, *15*, 166−173.
(35) Walcarius, A.; Minteer, S. D.; Wang, J.; Lin, Y. H.; Merkoci, A. Nanomaterials for Bio-Functionalized Electrodes: Recent Trends. *J. Mater. Chem. B* **2013**, *1*, 4878−4908.
(36) Liang, B. G. X.; Fang, L.; Hu, Y.; Yang, G.; Zhu, Q.; Wei, J.; Ye, X. Study of Direct Electron Transfer and Enzyme Activity of Glucose Oxidase on Graphene Surface. *Electrochem. Commun.* **2015**, *50*, 1−5.
(37) Kwon, C. H.; Lee, S. H.; Choi, Y. B.; Lee, J. A.; Kim, S. H.; Kim, H. H.; Spinks, G. M.; Wallace, G. G.; Lima, M. D.; Kozlov, M. E.; Baughman, R. H.; Kim, S. J. High-Power Biofuel Cell Textiles from Woven Biscrolled Carbon Nanotube Yarns. *Nat. Commun.* **2014**, *5*, 3928.
(38) Kuila, T.; Bose, S.; Khanra, P.; Mishra, A. K.; Kim, N. H.; Lee, J. H. Recent Advances in Graphene-Based Biosensors. *Biosens. Bioelectron.* **2011**, *26*, 4637−4648.
(39) Zhang, Y. J.; Chu, M.; Yang, L.; Tan, Y. M.; Deng, W. F.; Ma, M.; Su, X. L.; Xie, Q. J. Three-Dimensional Graphene Networks as a New Substrate for Immobilization of Laccase and Dopamine and Its Application in Glucose/O_2 Biofuel Cell. *ACS Appl. Mater. Interfaces* **2014**, *6*, 12808−12814.
(40) Brunauer, S.; Emmett, P. H.; Teller, E. Adsorption of Gases in Multimolecular Layers. *J. Am. Chem. Soc.* **1938**, *60*, 309−319.
(41) Kim, K. H.; Oh, Y.; Islam, M. F. Mechanical and Thermal Management Characteristics of Ultrahigh Surface Area Single-Walled Carbon Nanotube Aerogels. *Adv. Funct. Mater.* **2013**, *23*, 377−383.
(42) Kim, K. H.; Oh, Y.; Islam, M. F. Graphene Coating Makes Carbon Nanotube Aerogels Superelastic and Resistant to Fatigue. *Nat. Nanotechnol.* **2012**, *7*, 562−566.
(43) Bryning, M. B.; Milkie, D. E.; Islam, M. F.; Hough, L. A.; Kikkawa, J. M.; Yodh, A. G. Carbon Nanotube Aerogels. *Adv. Mater.* **2007**, *19*, 661−664.
(44) Islam, M. F.; Rojas, E.; Bergey, D. M.; Johnson, A. T.; Yodh, A. G. High Weight Fraction Surfactant Solubilization of Single-Wall Carbon Nanotubes in Water. *Nano Lett.* **2003**, *3*, 269−273.
(45) Hummers, W. S.; Offeman, R. E. Preparation of Graphitic Oxide. *J. Am. Chem. Soc.* **1958**, *80*, 1339−1339.
(46) Marcano, D. C.; Kosynkin, D. V.; Berlin, J. M.; Sinitskii, A.; Sun, Z. Z.; Slesarev, A.; Alemany, L. B.; Lu, W.; Tour, J. M. Improved Synthesis of Graphene Oxide. *ACS Nano* **2010**, *4*, 4806−4814.
(47) Chen, D. T. N.; Chen, K.; Hough, L. A.; Islam, M. F.; Yodh, A. G. Rheology of Carbon Nanotube Networks During Gelation. *Macromolecules* **2010**, *43*, 2048−2053.
(48) Hough, L. A.; Islam, M. F.; Janmey, P. A.; Yodh, A. G. Viscoelasticity of Single Wall Carbon Nanotube Suspensions. *Phys. Rev. Lett.* **2004**, *93*, 168102.
(49) Fan, F. R. F.; Bard, A. J. Imaging of Biological Macromolecules on Mica in Humid Air by Scanning Electrochemical Microscopy. *Proc. Natl. Acad. Sci. U. S. A.* **1999**, *96*, 14222−14227.
(50) Gong, C.; He, Y.; Zhou, J.; Chen, W.; Han, W.; Zhang, Z.; Zhang, P.; Pan, X.; Wang, Z.; Xie, E. Synthesis on Winged Graphene Nanofibers and Their Electrochemical Capacitive Performance. *ACS Appl. Mater. Interfaces* **2014**, *6*, 14844−14850.
(51) Heller, A. Miniature Biofuel Cells. *Phys. Chem. Chem. Phys.* **2004**, *6*, 209−216.
(52) Rabaey, K.; Boon, N.; Siciliano, S. D.; Verhaege, M.; Verstraete, W. Biofuel Cells Select for Microbial Consortia That Self-Mediate Electron Transfer. *Appl. Environ. Microbiol.* **2004**, *70*, 5373−5382.
(53) Campbell, A. S.; Dong, C. B.; Meng, F. K.; Hardinger, J.; Perhinschi, G.; Wu, N. Q.; Dinu, C. Z. Enzyme Catalytic Efficiency: A Function of Bio-Nano Interface Reactions. *ACS Appl. Mater. Interfaces* **2014**, *6*, 5393−5403.
(54) Laviron, E. General Expression of the Linear Potential Sweep Voltammogram in the Case of Diffusionless Electrochemical Systems. *J. Electroanal. Chem.* **1979**, *101*, 19−28.
(55) Rahimi, P.; Rafiee-Pour, H. A.; Ghourchian, H.; Norouzi, P.; Ganjali, M. R. Ionic-Liquid/NH_2-MWCNTs as a Highly Sensitive Nano-Composite for Catalase Direct Electrochemistry. *Biosens. Bioelectron.* **2010**, *25*, 1301−1306.
(56) Mani, V.; Devadas, B.; Chen, S. M. Direct Electrochemistry of Glucose Oxidase at Electrochemically Reduced Graphene Oxide-Multiwalled Carbon Nanotubes Hybrid Material Modified Electrode for Glucose Biosensor. *Biosens. Bioelectron.* **2013**, *41*, 309−315.
(57) Gao, Y. F.; Yang, T.; Yang, X. L.; Zhang, Y. S.; Xiao, B. L.; Hong, J.; Sheibani, N.; Ghourchian, H.; Hong, T.; Moosavi-Movahedi, A. A. Direct Electrochemistry of Glucose Oxidase and Glucose Biosensing on a Hydroxyl Fullerenes Modified Glassy Carbon Electrode. *Biosens. Bioelectron.* **2014**, *60*, 30−34.
(58) Razmi, H.; Mohammad-Rezaei, R. Graphene Quantum Dots as a New Substrate for Immobilization and Direct Electrochemistry of Glucose Oxidase: Application to Sensitive Glucose Determination. *Biosens. Bioelectron.* **2013**, *41*, 498−504.
(59) Wang, J. *Analytical Electrochemistry*, 2nd ed.; John Wiley & Sons: New York, 2000.
(60) Brocato, S.; Lau, C.; Atanassov, P. Mechanistic Study of Direct Electron Transfer in Bilirubin Oxidase. *Electrochim. Acta* **2012**, *61*, 44−49.
(61) Cracknell, J. A.; McNamara, T. P.; Lowe, E. D.; Blanford, C. F. Bilirubin Oxidase from *Myrothecium verrucaria*: X-ray Determination of the Complete Crystal Structure and a Rational Surface Modification for Enhanced Electrocatalytic O_2 Reduction. *Dalton Trans.* **2011**, *40*, 6668−6675.
(62) Ramasamy, R. P.; Luckarift, H. R.; Ivnitski, D. M.; Atanassov, P. B.; Johnson, G. R. High Electrocatalytic Activity of Tethered Multicopper Oxidase-Carbon Nanotube Conjugates. *Chem. Commun.* **2010**, *46*, 6045−6047.
(63) Christenson, A.; Shleev, S.; Mano, N.; Heller, A.; Gorton, L. Redox Potentials of the Blue Copper Sites of Bilirubin Oxidases. *Biochim. Biophys. Acta, Bioenerg.* **2006**, *1757*, 1634−1641.
(64) Shleev, S.; El Kasmi, A.; Ruzgas, T.; Gorton, L. Direct Heterogeneous Electron Transfer Reactions of Bilirubin Oxidase at a Spectrographic Graphite Electrode. *Electrochem. Commun.* **2004**, *6*, 934−939.
(65) Shleev, S.; Jarosz-Wilkolazka, A.; Khalunina, A.; Morozova, O.; Yaropolov, A.; Ruzgas, T.; Gorton, L. Direct Electron Transfer Reactions of Laccases from Different Origins on Carbon Electrodes. *Bioelectrochemistry* **2005**, *67*, 115−124.
(66) Ammam, M.; Fransaer, J. Combination of Laccase and Catalase in Construction of H_2O_2-O_2 based Biocathode for Applications in Glucose Biofuel Cells. *Biosens. Bioelectron.* **2013**, *39*, 274−281.

DOI: 10.1021/am507801x
ACS Appl. Mater. Interfaces 2015, 7, 4056−4065

(67) Zheng, W.; Zhao, H. Y.; Zhou, H. M.; Xu, X. X.; Ding, M. H.; Zheng, Y. F. Electrochemistry of Bilirubin Oxidase at Carbon Nanotubes. *J. Solid State Electrochem.* **2010**, *14*, 249−254.
(68) Devadas, B.; Mani, V.; Chen, S. M. A Glucose/O_2 Biofuel Cell Based on Graphene and Multiwalled Carbon Nanotube Composite Modified Electrode. *Int. J. Electrochem. Sci.* **2012**, *7*, 8064−8075.
(69) Palanisamy, S.; Cheemalapati, S.; Chen, S. M. An Enzymatic Biofuel Cell Based on Electrochemically Reduced Graphene Oxide and Multiwalled Carbon Nanotubes/Zinc Oxide Modified Electrode. *Int. J. Electrochem. Sci.* **2012**, *7*, 11477−11487.
(70) Dudzik, J.; Chang, W. C.; Kannan, A. M.; Filipek, S.; Viswanathan, S.; Li, P. Z.; Renugopalakrishnan, V.; Audette, G. F. Cross-Linked Glucose Oxidase Clusters for Biofuel Cell Anode Catalysts. *Biofabrication* **2013**, *5*, 035009.
(71) Shan, G. B.; Surampalli, R. Y.; Tyagi, R. D.; Zhang, T. C. Nanomaterials for Environmental Burden Reduction, Waste Treatment, and Nonpoint Source Pollution Control: A Review. *Front. Environ. Sci. Eng.* **2009**, *3*, 249−264.
(72) Schubart, I. W.; Gobel, G.; Lisdat, F. A Pyrroloquinolinequinone-Dependent Glucose Dehydrogenase (PQQ-GDH)-Electrode with Direct Electron Transfer Based on Polyaniline Modified Carbon Nanotubes for Biofuel Cell Application. *Electrochim. Acta* **2012**, *82*, 224−232.
(73) Min, K.; Ryu, J. H.; Yoo, Y. J. Mediator-Free Glucose/O_2 Biofuel Cell Based on a 3-Dimensional Glucose Oxidase/SWNT/Polypyrrole Composite Electrode. *Biotechnol. Bioprocess Eng.* **2010**, *15*, 371−375.
(74) Kwon, C. H.; Lee, S. H.; Choi, Y. B.; Lee, J. A.; Kim, S. H.; Kim, H. H.; Spinks, G. M.; Wallace, G. G.; Lima, M. D.; Kozlov, M. E.; Baughman, R. H.; Kim, S. J. High-Power Biofuel Cell Textiles from Woven Biscrolled Carbon Nanotube Yarns. *Nat. Commun.* **2014**, *5*, 3928.
(75) Deng, L.; Shang, L.; Wang, Y. Z.; Wang, T.; Chen, H. J.; Dong, S. J. Multilayer Structured Carbon Nanotubes/Poly-L-Lysine/Laccase Composite Cathode for Glucose/O_2 Biofuel Cell. *Electrochem. Commun.* **2008**, *10*, 1012−1015.
(76) Scherbahn, V.; Putze, M. T.; Dietzel, B.; Heinlein, T.; Schneider, J. J.; Lisdat, F. Biofuel Cells Based on Direct Enzyme-Electrode Contacts Using PQQ-Dependent Glucose Dehydrogenase/Bilirubin Oxidase and Modified Carbon Nanotube Materials. *Biosens. Bioelectron.* **2014**, *61*, 631−638.

DOI: 10.1021/am507801x
ACS Appl. Mater. Interfaces 2015, 7, 4056−4065